

Accelerated design of proton exchange membranes for green hydrogen production with artificial intelligence

Huan Tran,^{*,†,‡} Akhlak Mahmood,[†] Harshal Chaudhari,[¶] Kuldeep Mamtani,[¶]
Chiho Kim,^{†,‡} Rampi Ramprasad,^{†,‡} Anand N. Krishnamoorthy,^{*,¶} and Abhirup
Patra^{*,§}

[†]*Matmerize Inc., Atlanta, GA 30332, USA*

[‡]*School of Materials Science and Engineering, Georgia Institute of Technology, Atlanta,
GA 30332, USA*

[¶]*Shell India Put Ltd., Bengaluru, Karnataka, India*

[§]*Shell International Exploration and Production Inc., Houston, TX, USA*

E-mail: huan.tran@matmerize.com; A.NarayananKrishnam2@shell.com;
Abhirup.Patra@shell.com

Abstract

Water electrolysis is an eco-friendly method for hydrogen production that has reached significant levels of technological maturity. Among commercialized water-electrolysis technologies, proton-exchange membrane electrolyzers offer high current density, fast dynamic response, and compact system design, among other advantages. On the other hand, managing their high capital cost and the “forever-chemistry” nature of Nafion, a perfluorinated proton-exchange membrane widely used in such devices, remains a major challenge. Searches for fluorine-free replacements for Nafion, pursued largely through physical experimentation, have been active for decades with limited success. In this work, we develop and demonstrate an AI-based strategy for designing new proton-exchange membranes for electrolyzers. Two key components of this strategy are an implementation of the virtual forward-synthesis approach and a set of machine-learning predictive models for essential application-inspired membrane properties; the former generates a vast space of millions of synthesizable polymers, which are then evaluated and screened by the latter. The strategy is validated against experimental data for known membranes and then applied to design over 1,700 new synthesizable candidates. This article concludes with a forward-looking vision in which the strategy could be elevated into an interactive and iterative scheme that are based on large language models to facilitate materials design in multiple ways.

1 Introduction

Hydrogen is an ideal “fuel” that can be efficiently converted to multiple forms of end-use energy, e.g., electricity (using fuel cells) and mechanical energy (using hydrogen internal combustion engines).^{1–3} At the industrial scale, hydrogen is primarily produced from natural gases using steam reforming, gasification, and pyrolysis, during which a great volume of carbon dioxide is also generated.^{4,5} *Electrolysis*, the process in which water molecules are decomposed into hydrogen (H_2) and oxygen (O_2) gases using electrical energy, is a *green* method with essentially no carbon footprint.^{5–10} In an electrolytic cell, schematically shown in Fig. 1 (a), a direct current runs between the anode and cathode, driving two electrochemical reactions, i.e., oxygen evolution reaction (OER) and hydrogen evolution reaction (HER), that create H_2 and O_2 from water. An electrolyte layer sandwiched between the electrodes enables the transport of designated ions (e.g., H^+ or OH^-) while preventing the crossover of electrons, H_2 , and O_2 . Categorized by the cell architecture and electrolyte, major types electrolyzers are alkaline water electrolyzer, proton-exchange membrane (PEM) water electrolyzer, anion exchange membrane water electrolyzer, and solid oxide electrolysis cells.^{5,7} Technically, water electrolysis is scalable and insusceptible to the intermittency and variability of renewable electricity, typically generated from wind, solar, hydro, geothermal, and tidal sources. Toward a green future, this hydrogen production method is attractive for both commercial and policy reasons.⁹

PEM electrolyzers are a commercialized technology, offering high current density, fast dynamic response, high pressure operation, compact system design, and long lifetime.⁵ Compared to alkaline water electrolyzers, another mature technology,^{11,12} PEM electrolyzers are expensive because of their precious-metal electrocatalysts and proton-exchange membranes, typically Nafion [see Fig. 1(b)], known for its remarkable proton conductivity and durability under harsh working conditions. Beyond the capital cost considerations, recycling this per-fluorinated sulphonic acid copolymer is economically and environmentally highly unfavorable due to its superior stability, which arises from the exceptionally strong carbon-fluorine bonds

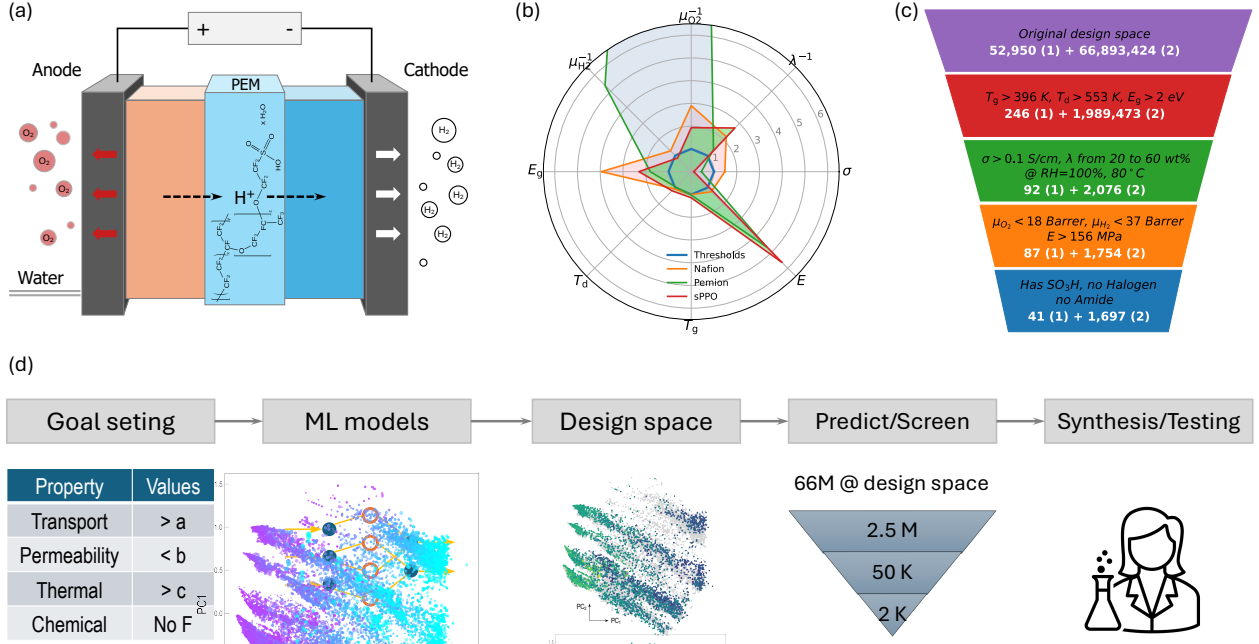


Figure 1: (a) A (schematic) cross-sectional view of a PEM electrolyzer in which a direct-current power source is used to split provided water molecules into hydrogen and oxygen gases in cathode and anode, (b) the chemical structure and a visualization of Nafion membrane, (c) the performances of Nafion, Pemion, and sPPO, given with respect to the application-inspired thresholds, and (d) the employed design strategy for PEMs. In (c), the design criteria are represented by a threshold polygon, outside of which good candidates for PEMs are expected to be.

dominating the membrane.^{5–10}

These long-standing issues motivate numerous active searches for sustainable (e.g., halogen-free), degradable, and more cost-effective PEMs during the last decades with limited successes.^{7,13–19} The primary challenge is that the polymer space is prohibitively large for traditional methods, typically relying on laborious and time-consuming physical experimentations and computer simulations. Artificial intelligence (AI)-based methods have also been developed and introduced,^{17–19} potentially accelerating the searches significantly. Among the identified, some halogen-free membranes, including Pemion^{20–22} and sulfonated poly(2,6-dimethyl-1,4-phenylene oxide) (sPPO),^{23–27} have been studied and even commercialized.^{28,29} Compared to Nafion, their proton conductivity, stability, and/or durability under working conditions, as shown in Fig. 1 (b), remain behind.^{20–22}

This paper describes an large-scale artificial intelligence (AI)-based effort to design new halogen-free PEMs for water electrolyzers. The employed strategy, visualized in Fig. 1 (d),^{17,18} involves creating a set of application-inspired property requirements for PEMs, developing machine-learning (ML) models to predict the properties,^{30,31} generating a massive design space of millions of polymers using virtual forward synthesis (VFS) approach,^{32–36} screening the space using the developed ML models for candidates, and testing them experimentally. After Nafion, Pemion, sPPO, and other sulfonate copolymers were “rediscovered” and validated, over 1,700 new synthetically-achievable polymers were identified from the screening, detailed in Fig. 1 (c). For some of them, synthesis and testing are on-going and results are anticipated. The described AI-based polymer design strategy could be leveraged to develop an interactive, iterative large language model based scheme for future polymer research and development.

2 Methods

2.1 Design criteria

The property requirements for water electrolyzer PEMs were crafted and summarized in Table 1. Among them, a *high* proton conductivity σ is critically important. Because proton transport requires the presence of water molecules and a network of inter-connected water channels in PEMs,^{37–41} the proton conductivity σ correlates strongly with the water uptake λ while both σ and λ are functions of the temperature T and the relative humidity RH of the working environment. For Nafion, high σ can only be reached when λ and RH are high, i.e., $\lambda \simeq 100$ wt% and RH $\simeq 100\%$, an undesirable requirement for practical operations.^{38,39,42} Therefore, a *moderate* level of water uptake λ , i.e., about 50 wt% or below is targeted. Then, as the water channels must withstand internal pressure to remain connected during the membrane’s lifetime, which could extend to tens of thousands of operating hours at $\simeq 80^\circ\text{C}$, PEMs should be mechanically strong and thermally robust. These requirements are

Table 1: Required performances of an electrolyzer’s proton exchange membrane. For Young’s modulus E , glass transition temperature T_g , thermal decomposition temperature T_d , O_2 permeability μ_{O_2} , and H_2 permeability μ_{H_2} , the thresholds reflect the actual performances of Nafion.

No.	Key property	Unit	Desired value	Nafion value
1	Proton conductivity σ	S/cm	$> 0.1 @ T = 80^\circ\text{C}$, RH=100%	$\simeq 0.1 @ T = 80^\circ\text{C}$, RH=100% ^{43–48}
2	Water uptake λ	wt%	< 50 wt%	> 50 wt% ^{44,47}
3	Young’s modulus E	MPa	> 156	$50 - 220$ ^{44,49,50}
4	Glass transition temperature T_g	K	> 396	$396 - 398$ ^{51,52}
5	Thermal decomposition temperature T_d	K	> 553	553 ^{53,54}
6	O_2 permeability μ_{O_2}	Barrer	< 18	$1.1 - 34.3$ ^{44,55–57}
7	H_2 permeability μ_{H_2}	Barrer	< 37	$9.3 - 65.0$ ^{44,55–57}
8	Electronic band gap E_g	eV	> 2.0	N/A
9	Having halogen species	N/A	No	Yes
10	Having amide $-\text{C}(=\text{O})\text{NH}-$	N/A	No	No
11	Having sulfonate $-\text{SO}_3^-$	N/A	Yes	Yes

translated into some thresholds that must be exceeded by the Young’s modulus E , the glass transition temperature T_g , and the thermal decomposition temperature T_d (see Table 1 for details).¹⁸

While promoting proton and water transports, the PEM layer in an electrolyzer should block the crossover of O_2 and H_2 gases. Therefore, the oxygen and hydrogen permeabilities, i.e., μ_{O_2} and μ_{H_2} , of a good PEM should be low. Likewise, a PEM must be electronically insulating, and this requirement could be translated into a large enough electronic “band gap” E_g . A high value of E_g is also needed to secure the electrochemical stability of the PEM.¹⁸ As a voltage of about 1.23 V (on top of $\simeq 2.0$ eV between the anode and cathode in working conditions) is theoretically needed to split water molecules into O_2 and H_2 ,⁵ a criterion of $E_g \geq 2.0$ eV was used in this work. For the Young’s modulus E , glass transition temperature T_g , thermal decomposition temperature T_d , oxygen permeability μ_{O_2} , and hydrogen permeability μ_{H_2} , the thresholds, given in Table 1, approximate the reported performances of Nafion.

Table 2: Summary of the dataset curated and the ML models trained on these datasets. The error metrics of the models are the coefficient of determination R^2 and either “root-mean-square error”, given by the same unit with the data, or “order of magnitude”, given by “order” and indicated by “ \underline{o} ”.

Property	Unit	Data size	Data range	R^2	Error
σ	S/cm	2,462	5×10^{-6} - 3.9×10^{-1}	0.84	0.12 \underline{o}
λ	wt%	2,120	0.03 - 2,500	0.96	0.10 \underline{o}
E	MPa	915	0.02 - 4,000	0.82	0.15 \underline{o}
T_g	K	8,962	80 - 873	0.99	10.0
T_d	K	6,585	291 - 1,173	0.96	21.9
μ_{O_2}	Barrett	1,021	1.5×10^{-8} - 1.9×10^4	0.95	0.07 \underline{o}
μ_{H_2}	Barrett	603	1.9×10^{-6} - 3.7×10^4	0.97	0.06 \underline{o}
E_g	eV	3,879	0.1-9.8	0.97	0.25

Some chemistry considerations were also considered for the design. First, avoiding halogen species is a primary objective, thus, the candidates should not have them. Then, amide groups $-C(=O)NH-$ tend to make strong hydrogen bonds with water molecules, trapping them, and limiting the proton mobility. They are also prone to hydrolysis and can be a site for radical-based degradation, leading to long-term degradation of the membranes, typically soaked in water. Therefore, amide groups should also be excluded. Finally, a vast majority of the proton conductivity σ and water uptake λ data reported in the literature and curated for this project contains sulfonate ($-SO_3^-$), the hydrophilic functional groups that are essential for capturing water molecules in the membranes (see Sec. 2.2).^{14,39,58} Consequently, we consider only candidates that have $-SO_3^-$ to make our σ and λ predictions reliable.

2.2 Training data and ML models

Table 2 provides a summary of the datasets prepared to train the necessary ML predictive models. The datasets of proton conductivity σ and water uptake λ , two strongly related properties, contain 2,462 and 2,120 data points, respectively. About 97.8% (2,409 entries) of the σ dataset and 48.7% (1,034 entries) of the λ dataset involve $-SO_3^-$ sulfonate group, highlighting the focus of the field in the last several decades. Likewise, two datasets of O_2 and H_2 permeabilities are parts a bigger dataset, containing 4,377 entries of the permeabilities

of six gases, including O_2 , H_2 , N_2 , He , CO_2 , a CH_4 . Except for the band gap E_g dataset that was prepared by using density functional density calculations,^{59–61} the other datasets are *experimental* in nature. Polymers in these datasets are represented by SMILES, which stands for *simplified molecular-input line-entry system*,⁶² from which a set of hierarchical chemical fingerprints^{30,31,63–65} will be computed for the development of the ML models. For proton conductivity σ and water uptake λ , the model development needs some additional descriptors, including the temperature T , the relative humidity RH, and another important measurement condition, i.e., whether the samples are submerged in liquid or vapor water.

We used Gaussian Process Regression,^{66,67} a similarity-based algorithm with a useful built-in measure of uncertainty and essentially zero inference time, to develop the necessary ML predictive models.^{30,31} As σ and λ are strongly correlated, a *multi-task* ML model was trained to predict both of them simultaneously. The rationale behind this solution is that for properties that are explicitly or implicitly related, multi-task algorithms are expected to exploit the possible correlations among them and make the models more robust and accurate.^{68–70} Likewise, another multi-task model was trained on the dataset combining the permeabilities of O_2 , H_2 , N_2 , He , CO_2 , a CH_4 for predicting μ_{O_2} and μ_{H_2} as needed for this strategy. Finally, four other ML models were trained to predict Young's modulus E , glass transition temperature T_g , thermal decomposition temperature T_d , and band gap E_g .

2.3 Design space

The design space (of homopolymers and copolymers) was constructed from about 30,000 known polymers,^{30,31} i.e., those that have been synthesized, studied, and reported, and about 66 millions synthesizable polymers generated using RxnChainer,³⁶ an implementation of the virtual forward synthesis (VFS) approach.^{32–35} In a nutshell, VFS starts with millions of commercially available monomers, which can be found from multiple sources, including TSCA inventory,⁷¹ ZINC-22,⁷² ChemBL,⁷³ and eMolecules.⁷⁴ These reactants are then propagated through numerous reaction chains, each of them is constructed from hun-

dreds of rule-based polymerization templates, such as step growth, chain-growth addition, ring-opening, and metathesis, to generate the product polymers. In other words, VFS mimics the real polymerization reactions to create highly synthesizable polymers. Given the vast number of available monomers^{71–74} and polymerization templates,^{34,35} the number of polymers that can be generated using this approach is essentially unlimited.^{32–35}

The considered design space contains nearly 66 millions syntherizable and/or synthesized polymers, categorized into 2 subsets. Subset 1 has 52,950 polymers, including 26,958 polymer that have been synthesized, studied, and reported in the literature,^{30,31} and 25,992 copolymers generated from known homopolymers. Subset 2 is much bigger, encompassing 66,893,424 homopolymers and copolymers generated from more than 7 millions commercial monomers obtained from TSCA inventory.⁷¹ For practical reasons, four typical polymer families, namely polyimides, polyesters, polyureas, and polyurethanes, were considered for subset 2.

Results reported herein, including model training, design space creation, and the subsequent candidate screening (based on the established design criteria), were performed using PolymRizeTM, a cloud-based polymer informatics software.⁷⁵

3 Results

3.1 Machine-learning models

The training process of the ML models is summarized in Table 2. Each trained ML model is characterized by a coefficient of determination R^2 and an error measure, which, depending on the training data distribution, can either be the root-mean-square error (RMSE) of the *order of magnitude error* (OME). For T_g , T_d , and E_g , the data range is not too large, i.e., the upper bound is about 10 times of the lower bound or less, RMSE was used. On the other hand, as the data of σ , λ , E , μ_{O_2} , and μ_{H_2} are highly scattered, i.e., spanning for 4-6 order of magnitudes, OME is a more suitable error metric. Formally, OME is defined

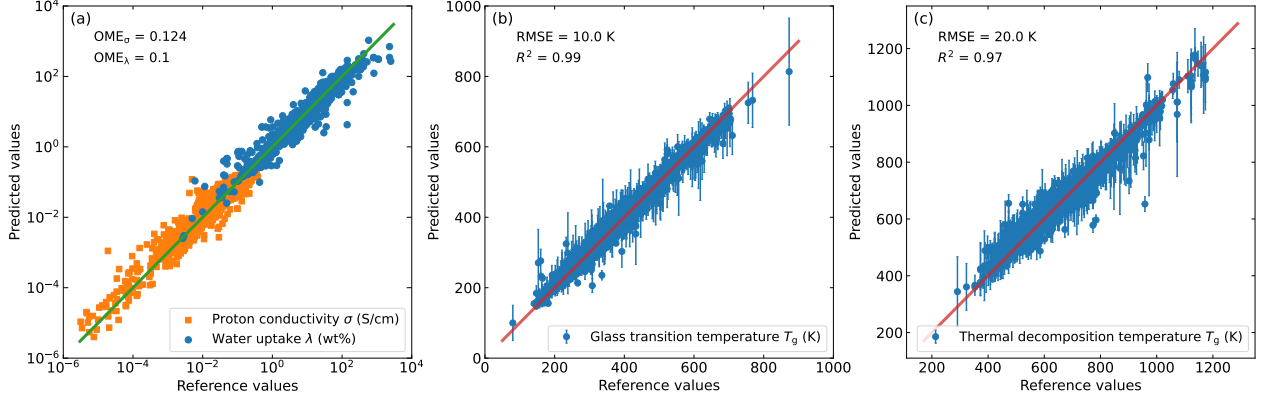


Figure 2: ML models for (a) proton conductivity and water uptake, (b) glass transition temperature, and (c) thermal decomposition temperature.

as $\langle \text{abs}(\log_{10}(p_{\text{pred}}/p_{\text{ref}})) \rangle$, where p_{pred} and p_{ref} are the predicted and reference values and $\langle \dots \rangle$ stand for the average over the predictions. With this definition, OME provides the anticipated error of the predictions, given in “orders of magnitude” and denoted by $\underline{\text{o}}$. Both RMSE and OME should be examined in comparison with the range of the training data.

The coefficient of determination R^2 of all the models is high. Except for σ and E models whose R^2 is 0.84 and 0.82, respectively, $R^2 > 0.95$ for other models. Two error measures, namely RMSE and OME, are small. In particular, RMSE obtained for T_g , T_d , and E_g models is about 3-7% of the training data range while OME is about $0.1\underline{\text{o}}$ for all the ML models developed for σ , λ , E , μ_{O_2} , and μ_{H_2} . This error measure is roughly 3-5% of the training data range, which is about $4\text{-}6\underline{\text{o}}$. Fig. 2 provides a visualization of the models trained for predicting λ , σ , T_g , and T_d .

3.2 Discovered PEM candidates

As visualized in Figs. 1 (c), a set of 1,738 candidates for electrolyzer PEMs were down-selected from the original design space, containing 41 polymers in subset 1 and 1,697 polymers (136 polyesters and 1,569 polyimides) in subset 2. While our experimental tests for sPPO were completed, synthesis and testing works for some other candidates are ongoing, and results may be anticipated.

3.2.1 Known membranes: experimental validations

Among the polymers identified from subset 1, Nafion, Pemion, and PPO are examined in Figs. 3 (b), (c), and (d) with respect to available measured data. In Figs. 3 (b) and (c), the predicted proton conductivity captures very well the order and the trend of the experimental data reported for Nafion⁴³⁻⁴⁸ and Pemion,^{20,28} giving an excellent overall accuracy. For sPPO, we performed necessary measurements on commercial membranes (InnoSep-C) acquired from Innochemtech Inc.²⁹ Using a BT-110 conductivity clamp, our electrochemical impedance spectroscopy measurements were performed to determine the high-frequency resistance R at temperature ranging from 24 to 90°C. Then, the in-plane proton conductivity σ was calculated using $\sigma = L/Rwt$ where L is the distance between the reference electrodes while w and t are the width and thickness of the membrane. The measured data is given Fig. 3 (d), also providing a compelling confirmation of our ML predictions.

Ref. 76 claims several series of sulfonated aromatic poly(ether sulfone) colymers (SPAES), for one of them the generic chemical structure is shown in Figs. 3 (d) and (e). In this series, Y may come from a group consisting of -S-, S(O), -S(O)₂-, -C(O)-, -P(O)(C₆H₅)- and their combinations, Z may come from a group consisting of -C(CH₃)₂-, -C(CF₃)₂-, -C(CF₃)(C₆H₅)-, -C(O)-, -S(O)₂-, or -P(O)(C₆H₅)-, while $n/(m+n)$ may range from 0.001 to 1.⁷⁶ By screening over all the non-halogen possibilities, we identified 2 candidates, denoted by SPAES1 and SPAES2, that meet our design criteria. SPAES1 includes -S- block for Y, -SO₂- block for Z, and $n/(m+n) = 0.3$, while for SPAES2, Y is -S-, Z is -C(=O)-, and $n/(m+n) = 0.3$.

The predicted water uptake of Nafion is shown in Figs. 3 (f). Compared to the measured data, obtained from Refs. 44,47, the predictions capture well both the order of magnitude and the trend of this important property, given as a function of the relative humidity. Nevertheless, the predictions shown in Figs. 3 (c)-(f) feature relatively high uncertainty, implying that the proton conductivity and water uptake models have not been exposed to enough volume of related data, and their training data should further be augmented. All the data predicted and measured for other properties are summarized in Table 3.

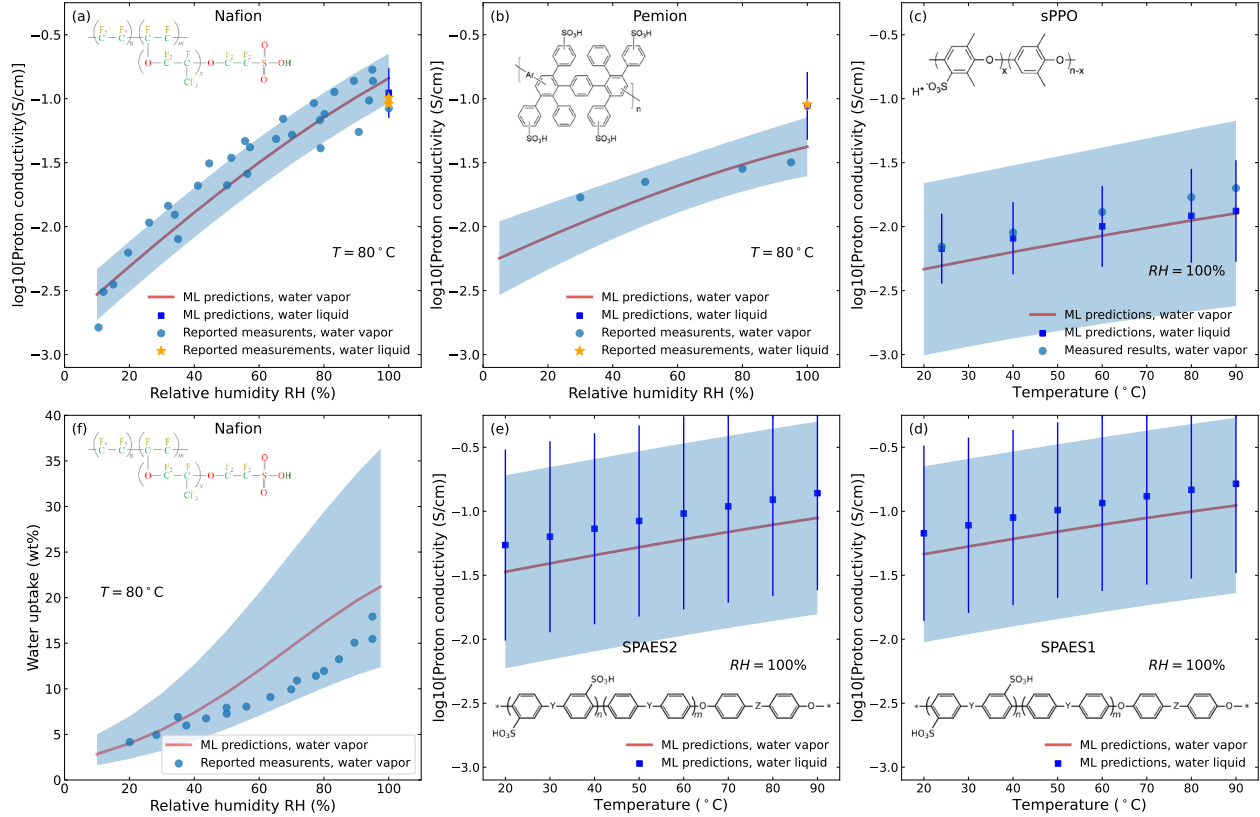


Figure 3: Chemical structure and predicted proton conductivity (a) and water uptake (b) of Nafion, given in comparison with experimental data, taken from Refs. 43–48 and Refs. 44,47, respectively. In (b), (c), (d), and (e), the predicted proton conductivity of Pemion, sPPO, and 2 sulfonated aromatic poly(ether sulfone) copolymers SPAES1 and SPAES2 are given. Measured proton conductivity of Pemion was taken from Refs. 20,28. For sPPO, $x = 0.2$ and data were measured in this work. In SPAES1, Y is $-S-$, Z is $-SO_2-$, and $n/(m+n) = 0.3$, while for SPAES2, Y is $-S-$, Z is $-C(=O)-$, and $n/(m+n) = 0.3$. Shaded areas in panels (b)–(f) represent the uncertainty of the predictions for “water vapor” (given in solid lines).

Table 3 summarizes the predictions for other required performances of Nafion, Pemion, sPPO, SPAES1, and SPAES2. While the good agreement between the predicted and measured data of Nafion resembles our recent report,¹⁸ similar agreements can also be found for Pemion and sPPO. The predicted glass transition temperature $T_g = 485 \pm 26$ K and thermal decomposition temperature $T_d = 619 \pm 59$ K agree very well with experimental values, namely $T_g = 483$ K²⁷ and $T_d = 682$ K.⁷⁹ The prediction of Young’s modulus $E = 746 \pm 0.80$ MPa has no apparent experimental counterpart, but there is a report⁸³ on three sulfonated polyphenylene-based copolymers with similar rigid backbone with reason-

Table 3: Summary of the agreements between predicted and measured data of Nafion, Pemion, and sPPO. References are given for the experimental data collected from the literature.

Property	Nafion		Pemion		sPPO		SPAES1	SPAES2
	Measured	Predicted	Measured	Predicted	Measured	Predicted	Predicted	Predicted
E (MPa)	50-220 ^{44,49,50}	195 ± 0.4 ₀	405-930 ⁷⁷	729 ± 0.6 ₀	N/A	880 ± 0.7 ₀	$1,060 \pm 0.8$ ₀	$1,104 \pm 0.8$ ₀
T_g (K)	396-398 ^{51,52}	369 ± 32	> 393 ⁷⁸	408 ± 33	463 ± 17 ^{27,79}	455 ± 13	516 ± 46	517 ± 45
T_d (K)	553 ^{53,54}	589 ± 18	> 533 ⁸⁰	529 ± 10	682 ⁷⁹	658 ± 18	622 ± 48	624 ± 47
μ_{O_2} (Barrer)	$1.1\text{-}34.3$ ^{44,55-57}	6.2 ± 0.5 ₀	$\lesssim 0.1\mu_{O_2}^{\text{Naf}}$ ⁸¹	0.3 ± 1.5 ₀	6.4 ⁸²	9.3 ± 0.6 ₀	0.1 ± 1.7 ₀	0.1 ± 1.7 ₀
μ_{H_2} (Barrer)	$9.3\text{-}65.0$ ^{44,55-57}	28.7 ± 0.4 ₀	$\lesssim 0.1\mu_{H_2}^{\text{Naf}}$ ⁸¹	6.9 ± 0.9 ₀	30.9 ⁸²	43.6 ± 0.3 ₀	4.0 ± 1.0 ₀	4.1 ± 1.0 ₀
E_g (eV)	N/A	7.9 ± 0.2	N/A	3.6 ± 0.5	N/A	4.6 ± 0.4	3.3 ± 0.3	3.3 ± 0.3

able measured Young's modulus of $E \simeq 1,100$ MPa. Likewise, within an uncertainty of about $0.3 - 0.6$ ₀ (see Table 2), the predicted μ_{O_2} and μ_{H_2} are reasonably good compared to the experimental values. The predicted band gap $E_g = 4.6 \pm 0.4$ eV indicates that sPPO is a good insulating material that could be suitable for the harsh working conditions of an electrolyzer.

3.2.2 Uncharted territory: PEM candidates

Beyond the known polymers identified and validated in Sec. 3.2.1, the subset of 1,697 candidates identified from the essentially unexplored space of 66M generated polymers are expected to yield interesting and useful discoveries. While experimental synthesis and testing for some of them are ongoing, we analyzed their chemical structure for critical functional groups and chemical features.

Starting from the design criteria, more than 50 functional groups (blocks) that may be relevant to any property were compiled. The chemical structure of the candidates, given in their SMILES, was then examined, returning 10 most-frequent blocks shown in Fig. 4. Except sulfonate, which is required, phenyl (C_6H_5-) and 1,4-phenylene ($-C_6H_4-$) groups were found in every candidate, while biphenyl ($-C_6H_4-C_6H_4-$) occurs in 86% of them. The very high rotational barrier of 1,4-phenylene and the bulky, rigid phenyl side group strongly suppress segmental mobility and raise the glass transition temperature T_g . Likewise, $C(sp^2)-C(sp^2)$ and aromatic C-H bonds are strong with high bond-dissociation energies (~ 110 kcal/mol,

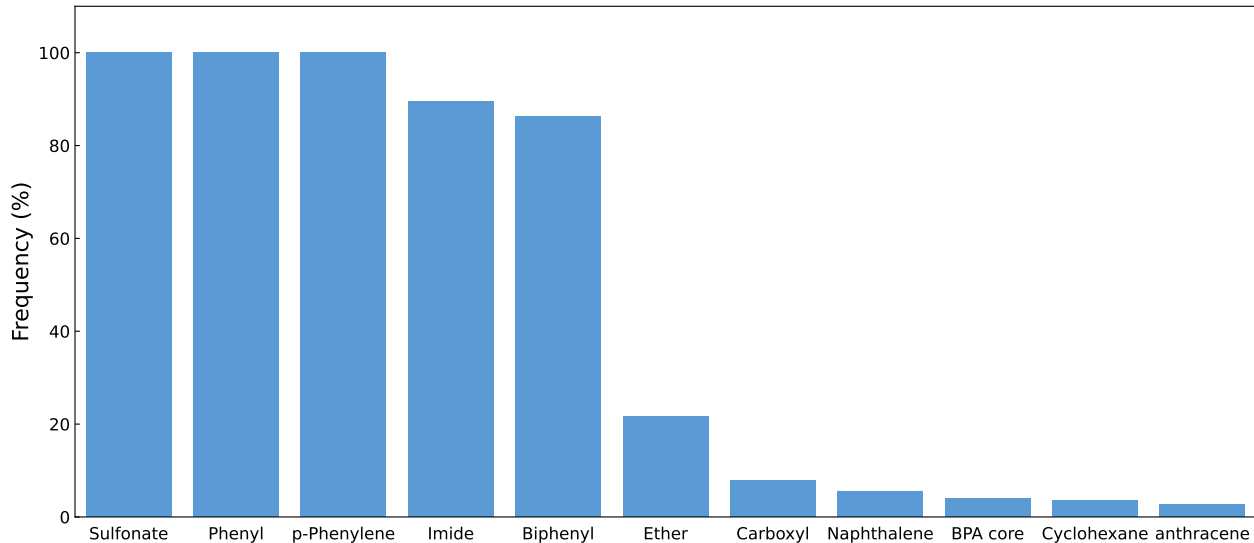


Figure 4: Ten most-frequent functional groups/blocks found in 1,738 candidates identified from subset 2, containing 66M polymers generated using VFS.

versus ~ 100 kcal/mol for aliphatic sp^3 bonds), thereby increasing the thermal decomposition temperature T_d . Moreover, the quasi-planar geometry of phenyl and 1,4-phenylene also promotes tighter packing, limiting the crossover of gases such as O_2 and H_2 , as required for a PEM. The imide group ($-\text{CO}-\text{NH}-\text{CO}-$), present in 89% of the candidate set, possesses dipoles that improve cohesion and the thermal and mechanical properties of the membranes. Overall, sulfonate, phenyl, 1,4-phenylene, biphenyl, and imide are the most important groups of our candidate set, reasonably and collectively promoting the critical properties required for electrolyzer PEMs.

4 Outlooks

The AI-based application-driven design strategy is inherently generic, opening several avenues for future polymer research and development. A particularly promising direction is the development of a large-language-model-based (AI) agent that integrates multi-objective optimization algorithms with the demonstrated VFS-ML workflow to enable interactive and application-driven polymer design. In this envisioned framework, users will interact with an

Interactive AI Agent for Materials Design

<p>USER: I need a halogen-free membrane with proton conductivity like Nafion but with improved mechanical strength at elevated temperatures. Can you help me?</p>	<p>USER: The glass transition temperature should be even higher, something above 500 K. Also, can you focus on polyimide-based structures?</p>	<p>USER: Awesome, yes, please export the top 3 candidates. Also show me the chemical structures.</p>
<p>AI AGENT: <i>Sure, I can help you with that. I'll translate your requirements into design criteria:</i></p> <ul style="list-style-type: none"> • Proton conductivity $\sigma > 0.1 \text{ S/cm}$ at 80°C • Young's modulus $E > 200 \text{ MPa}$ (Nafion: $\sim 156 \text{ MPa}$) • Glass transition temperature $T_g > 450 \text{ K}$ • No halogen species (F, Cl, Br, I) • Sulfonate groups ($-\text{SO}_3^-$) required for proton transport <p><i>Generating candidates using RxnChainer from 7M+ commercial monomers...</i></p> <ul style="list-style-type: none"> ✓ Generated 45,231 halogen-free polymers ✓ Screening with ML models... <p><i>Top 5 candidates found:</i></p> <ol style="list-style-type: none"> 1. Sulfonated polyimide-phenylene ($\sigma = 0.14 \text{ S/cm}$, $E = 285 \text{ MPa}$, $T_g = 512 \text{ K}$) 2. Sulfonated poly(arylene ether ketone) ($\sigma = 0.12 \text{ S/cm}$, $E = 245 \text{ MPa}$, $T_g = 478 \text{ K}$) 3. Sulfonated polybenzimidazole ($\sigma = 0.11 \text{ S/cm}$, $E = 312 \text{ MPa}$, $T_g = 531 \text{ K}$) <p><i>Would you like to refine the search criteria?</i></p>	<p>AI AGENT: <i>Adjusting criteria:</i></p> <ul style="list-style-type: none"> • $T_g > 500 \text{ K}$ (updated from 450 K) • Backbone must contain imide groups • Maintaining other constraints... <p><i>Re-screening design space...</i></p> <ul style="list-style-type: none"> ✓ 3,847 polyimide candidates identified <p><i>Top 2 refined candidates:</i></p> <ol style="list-style-type: none"> 1. Sulfonated poly(naphthalene-imide) ($\sigma = 0.13 \text{ S/cm}$, $E = 298 \text{ MPa}$, $T_g = 527 \text{ K}$, uncertainty: $\pm 15 \text{ K}$) 2. Sulfonated poly(biphenyl-imide) ($\sigma = 0.12 \text{ S/cm}$, $E = 315 \text{ MPa}$, $T_g = 518 \text{ K}$, uncertainty: $\pm 18 \text{ K}$) <p><i>Recommendation for experimental validation:</i></p> <p>Candidate #1 (low uncertainty, better property balance) and Candidate #2 (high mechanical strength)</p> <p><i>Export these candidates as a report?</i></p>	<p>AI AGENT:</p> <ul style="list-style-type: none"> ✓ Synthesis protocols gathered based on available monomers from the TSCA inventory ✓ Exported to synthesis data with full characterization report [PDF file] ✓ Chemical structures exported [structure diagrams] <p><i>Next steps:</i></p> <ul style="list-style-type: none"> • Experimental synthesis and testing recommended <p><i>Would you like to explore additional design spaces or modify constraints further?</i></p>

Figure 5: Schematic illustration of the envisioned interactive AI agent workflow for application-driven polymer design. User specify performance requirements through a natural language interface, the AI agent translates the requirements into quantitative design criteria, generates polymer candidates using RxnChainer (VFS approach), predicts their properties using trained ML models, and engages in iterative refinement loop based on user feedback. The agent provides explanations of structure-property relationships and presents ranked candidates with predicted property values, uncertainty estimates, and synthesizability scores.

AI agent through a natural language chat interface, specifying the desired performance metrics, constraints, and other requirements in conversational terms rather than through rigid parameter inputs. For example, a user may request “a halogen-free membrane with proton conductivity similar to Nafion but with improved mechanical strength at elevated temperatures.” The AI agent would then parse the requirements, translate them into quantitative design criteria, e.g., $\sigma > 0.1 \text{ S/cm}$ at 80°C , $E > 200 \text{ MPa}$, $T_g > 450 \text{ K}$, and leverage the VFS-ML framework to generate and evaluate the candidate materials.

An example of such an interaction is illustrated in Fig. 5. Having an user request, the agent would utilize RxnChainer,³⁶ an implementation of the VFS approach, to generate new polymer candidates from the vast space of commercially available monomers, applying the user-specified chemical constraints (e.g., excluding halogen species, requiring sulfonate

groups). The candidates would then be screened using the trained ML models to predict their properties. Critically, the agent would not simply return a ranked list of candidates but also engage in an iterative refinement process based on user feedback. If the initial candidates do not meet expectations, the user could provide additional guidance, e.g., “increase the glass transition temperature threshold” or “focus on polyimide-based structures”, and the agent would adjust the search accordingly. Throughout this process, the agent would provide explanations of the underlying structure-property relationships, highlighting which chemical moieties contribute to specific properties. For instance, it might explain that “the presence of rigid aromatic rings in the backbone enhances T_g and E , while the sulfonate side groups enable high σ through water uptake.”

Finally, the agent could also suggest experimental validation priorities based on the prediction uncertainties and potential impact. This interactive, iterative approach could transform the polymer design process from a one-time screening exercise into a dynamic collaboration between human expertise and AI capabilities. Such an intelligent framework could significantly accelerate the discovery of high-performance materials not only for PEMs but for a broad range of functional polymer applications, making advanced materials design accessible to researchers without extensive ML expertise.

5 Summary

We have demonstrated an AI-based, application-driven design scheme to develop sustainable (halogen-free) proton-exchange membranes for PEM electrolyzers. Central to this strategy are a virtual forward-synthesis approach, used to generate a large design space of synthesizable polymers, and a set of ML predictive models developed to evaluate candidates within this space. The ML models were validated against experimental data curated and/or generated for Nafion, Pemion, and sPPO. The strategy was then used to discover 1,738 promising PEM candidates, some of which are undergoing experimental synthesis and testing, with

further results anticipated. This strategy also suggests avenues for future polymer research and development. A particularly promising direction is the development of an AI agent that enables seamless interactions between users and the demonstrated AI-based strategy, fostering interactive and iterative human–machine collaboration for accelerated materials design.

Acknowledgement

This work was done within the GameChanger Initiative of Shell. The authors extend their sincere appreciation to Sreenivas Raghavendran for discussions and supports throughout the project. They gratefully acknowledge Innochemtech Co. Ltd., Republic of Korea, for generously providing the membrane samples free of charge, and especially Dr. Won-keun Son (CEO), Ji-won Kim, and Dr. S. Kumar for their support and coordination. The authors would also like to thank Sajanikumari Sadasivan and Cor van Kruijsdijk for their guidance on domain expertise.

Notes Competing interests: The authors declare no competing financial interests.

References

- (1) Züttel, A.; Remhof, A.; Borgschulte, A.; Friedrichs, O. Hydrogen: the future energy carrier. *Philos. Trans. A or Phil. Trans. R. Soc. A* **2010**, *368*, 3329–3342.
- (2) Abdalla, A. M.; Hossain, S.; Nisfindy, O. B.; Azad, A. T.; Dawood, M.; Azad, A. K. Hydrogen production, storage, transportation and key challenges with applications: A review. *Energy Convers. Manag.* **2018**, *165*, 602–627.
- (3) Akal, D.; Öztuna, S.; Büyükkakin, M. K. A review of hydrogen usage in internal com-

bustion engines (gasoline-Lpg-diesel) from combustion performance aspect. *Int. J. Hydrogen Energy* **2020**, *45*, 35257–35268.

(4) Mazloomi, K.; Gomes, C. Hydrogen as an energy carrier: Prospects and challenges. *Renew. Sustain. Energy Rev.* **2012**, *16*, 3024–3033.

(5) Kumar, S. S.; Lim, H. An overview of water electrolysis technologies for green hydrogen production. *Energy Rep.* **2022**, *8*, 13793–13813.

(6) Mansilha, C.; Barbosa-Póvoa, A.; Tarelho, L.; Fonseca, A. A comprehensive review of green hydrogen production technologies: current status, challenges, research trends and future directions. *Renew. Sustain. Energy Rev.* **2026**, *225*, 116119.

(7) Chatenet, M.; Pollet, B. G.; Dekel, D. R.; Dionigi, F.; Deseure, J.; Millet, P.; Braatz, R. D.; Bazant, M. Z.; Eikerling, M.; Staffell, I. et al. Water electrolysis: from textbook knowledge to the latest scientific strategies and industrial developments. *Chem. Soc. Rev.* **2022**, *51*, 4583–4762.

(8) Bodard, A.; Chen, Z.; ELJarray, O.; Zhang, G. Green Hydrogen Production by Low-Temperature Membrane-Engineered Water Electrolyzers, and Regenerative Fuel Cells. *Small Methods* **2024**, *8*, 2400574.

(9) Wang, C. R.; Stansberry, J. M.; Mukundan, R.; Chang, H.-M. J.; Kulkarni, D.; Park, A. M.; Plymill, A. B.; Firas, N. M.; Liu, C. P.; Lang, J. T. et al. Proton exchange membrane (PEM) water electrolysis: cell-level considerations for gigawatt-scale deployment. *Chem. Rev.* **2025**, *125*, 1257–1302.

(10) Nagao, Y. Proton-conducting polymers: key to next-generation fuel cells, electrolyzers, batteries, actuators, and sensors. *ChemElectroChem* **2024**, *11*, e202300846.

(11) Krishnan, S.; Koning, V.; de Groot, M. T.; de Groot, A.; Mendoza, P. G.; Junginger, M.;

Kramer, G. J. Present and future cost of alkaline and PEM electrolyser stacks. *Int. J. Hydrogen Energy* **2023**, *48*, 32313–32330.

(12) Hubert, M.; Esposito, A.; Peterson, D.; Miller, E.; Stanford, J. *Hydrogen Shot: Water Electrolysis Technology Assessment*; US Department of Energy, 2024.

(13) Miyake, J.; Taki, R.; Mochizuki, T.; Shimizu, R.; Akiyama, R.; Uchida, M.; Miyatake, K. Design of Flexible Polyphenylene Proton-Conducting Membrane for Next-Generation Fuel Cells. *Sci. Adv.* **2017**, *3*, eaao0476.

(14) Souzy, R.; Ameduri, B.; Boutevin, B.; Capron, P.; Marsacq, D.; Gebel, G. Proton-Conducting Polymer Electrolyte Membranes Based on Fluoropolymers Incorporating Perfluorovinyl Ether Sulfonic Acids and Fluoroalkenes: Synthesis and Characterization. *Fuel Cells* **2005**, *5*, 383–397.

(15) Wang, Y.; Seo, B.; Wang, B.; Zamel, N.; Jiao, K.; Adroher, X. C. Fundamentals, Materials, and Machine Learning of Polymer Electrolyte Membrane Fuel Cell Technology. *Energy and AI* **2020**, *1*, 100014.

(16) Kraytsberg, A.; Ein-Eli, Y. Review of Advanced Materials for Proton Exchange Membrane Fuel Cells. *Energy & Fuels* **2014**, *28*, 7303–7330.

(17) Tran, H.; Gurnani, R.; Kim, C.; Pilania, G.; Kwon, H.-K.; Lively, R. P.; Ramprasad, R. Design of functional and sustainable polymers assisted by artificial intelligence. *Nat. Rev. Mater.* **2024**, *9*, 866–886.

(18) Tran, H.; Shen, K.-H.; Shukla, S.; Kwon, H.-K.; Ramprasad, R. Informatics-Driven Selection of Polymers for Fuel-Cell Applications. *J. Phys. Chem. C* **2023**, *127*, 977–986.

(19) Schertzer, W.; Shukla, S.; Sose, A.; Rafiq, R.; Al Otmi, M.; Sampath, J.; Lively, R. P.;

Ramprasad, R. AI-driven design of fluorine-free polymers for sustainable and high-performance anion exchange membranes. *J. Mater. Infor.* **2025**, *5*, N–A.

(20) Nguyen, H.; Lombeck, F.; Schwarz, C.; Heizmann, P. A.; Adamski, M.; Lee, H.-F.; Britton, B.; Holdcroft, S.; Vierrath, S.; Breitwieser, M. Hydrocarbon-based PemionTM proton exchange membrane fuel cells with state-of-the-art performance. *Sustain. Energ. Fuels* **2021**, *5*, 3687–3699.

(21) Nguyen, H.; Klose, C.; Metzler, L.; Vierrath, S.; Breitwieser, M. Fully hydrocarbon membrane electrode assemblies for proton exchange membrane fuel cells and electrolyzers: An engineering perspective. *Adv. Energ. Mater.* **2022**, *12*, 2103559.

(22) Mirfarsi, S. H.; Kumar, A.; Jeong, J.; Adamski, M.; McDermid, S.; Britton, B.; Kjeang, E. High-temperature stability of hydrocarbon-based Pemion[®] proton exchange membranes: A thermo-mechanical stability study. *Int. J. Hydrogen Energy* **2024**, *50*, 1507–1522.

(23) Ashcraft, J. N.; Argun, A. A.; Hammond, P. T. Structure-property studies of highly conductive layer-by-layer assembled membranes for fuel cell PEM applications. *J. Mater. Chem.* **2010**, *20*, 6250–6257.

(24) Afsar, N. U.; Ji, W.; Wu, B.; Shehzad, M. A.; Ge, L.; Xu, T. SPPO-based cation exchange membranes with a positively charged layer for cation fractionation. *Desalination* **2019**, *472*, 114145.

(25) Khan, M. I.; Shanableh, A.; Shahida, S.; Lashari, M. H.; Manzoor, S.; Fernandez, J. SPEEK and SPPO blended membranes for proton exchange membrane fuel cells. *Membranes* **2022**, *12*, 263.

(26) Lee, J.-H.; Lee, J.-Y.; Kim, J.-H.; Joo, J.; Maurya, S.; Choun, M.; Lee, J.; Moon, S.-H. SPPO pore-filled composite membranes with electrically aligned ion channels via

a lab-scale continuous caster for fuel cells: An optimal DC electric field strength-IEC relationship. *J. Membr. Sci.* **2016**, *501*, 15–23.

(27) Nagendra, B.; Salman, S.; Peter Bloch, H.; Daniel, C.; Rizzo, P.; Fittipaldi, R.; Guerra, G. Poly (phenylene oxide) films with hydrophilic sulfonated amorphous phase and physically cross-linking hydrophobic crystalline phase. *ACS Appl. Polym. Mater.* **2023**, *5*, 3489–3498.

(28) Ionomr, *Pemion Fuel Cell Offerings Proton Exchange Membranes & Polymers*; 2021; PF1-HLF8-15-X, Document ID: FM-6027-B.

(29) Innochemtech Inc. <http://innochemtech.com/>.

(30) Kim, C.; Chandrasekaran, A.; Huan, T. D.; Das, D.; Ramprasad, R. Polymer Genome: A Data-Powered Polymer Informatics Platform for Property Predictions. *J. Phys. Chem. C* **2018**, *122*, 17575–17585.

(31) Tran, H.; Kim, C.; Chen, L.; Chandrasekaran, A.; Batra, R.; Venkatram, S.; Kamal, D.; Lightstone, J. P.; Gurnani, R.; Shetty, P. et al. Machine-Learning Predictions of Polymer Properties with Polymer Genome. *J. Appl. Phys.* **2020**, *128*, 171104.

(32) Kim, S.; Schroeder, C. M.; Jackson, N. E. Open macromolecular genome: Generative design of synthetically accessible polymers. *ACS Polymers Au* **2023**, *3*, 318–330.

(33) Ohno, M.; Hayashi, Y.; Zhang, Q.; Kaneko, Y.; Yoshida, R. SMiPoly: generation of a synthesizable polymer virtual library using rule-based polymerization reactions. *J. Chem. Infor. Model.* **2023**, *63*, 5539–5548.

(34) Gurnani, R.; Shukla, S.; Kamal, D.; Wu, C.; Hao, J.; Kuenneth, C.; Aklujkar, P.; Khomane, A.; Daniels, R.; Deshmukh, A. A. et al. AI-assisted discovery of high-temperature dielectrics for energy storage. *Nat. Commun.* **2024**, *15*, 6107.

(35) Kern, J.; Su, Y.-L.; Gutekunst, W.; Ramprasad, R. An informatics framework for the design of sustainable, chemically recyclable, synthetically accessible, and durable polymers. *npj Comput. Mater.* **2025**, *11*, 182.

(36) Shukla, S. S.; Kim, C.; Gurnani, R.; Ramprasad, R.; Mahmood, A. Stalking the Synthetically-Accessible Polymer Universe: Virtual Synthesis, Retrosynthesis and Beyond. *in preparation* **2025**,

(37) Li, X. *Principles of Fuel Cells*; CRC press, 2005.

(38) Jiao, K.; Li, X. Water Transport in Polymer Electrolyte Membrane Fuel Cells. *Prog. Energy Combust. Sci.* **2011**, *37*, 221–291.

(39) Kusoglu, A.; Weber, A. Z. New Insights into Perfluorinated Sulfonic-Acid Ionomers. *Chem. Rev.* **2017**, *117*, 987–1104.

(40) Kusoglu, A.; Weber, A. Z. *Polymers for Energy Storage and Delivery: Polyelectrolytes for Batteries and Fuel Cells*; ACS Publications, 2012; Chapter 11, pp 175–199.

(41) Hickner, M.; Pivovar, B. The Chemical and Structural Nature of Proton Exchange Membrane Fuel Cell Properties. *Fuel cells* **2005**, *5*, 213–229.

(42) Zhu, L.-Y.; Li, Y.-C.; Liu, J.; He, J.; Wang, L.-Y.; Lei, J.-D. Recent Developments in High-Performance Nafion Membranes for Hydrogen Fuel Cells Applications. *Pet. Sci.* **2022**, *19*, 1371.

(43) Feng, S.; Kondo, S.; Kaseyama, T.; Nakazawa, T.; Kikuchi, T.; Selyanchyn, R.; Fujikawa, S.; Christiani, L.; Sasaki, K.; Nishihara, M. Characterization of Polymer-Polymer Type Charge-Transfer (CT) Blend Membranes for Fuel Cell Application. *Data Br.* **2018**, *18*, 22–29.

(44) Zhang, Y.; Miyake, J.; Akiyama, R.; Shimizu, R.; Miyatake, K. Sulfonated Phenylene/Quinquephenylene/Perfluoroalkylene Terpolymers as Proton Exchange Membranes for Fuel Cells. *ACS Appl. Energy Mater.* **2018**, *1*, 1008–1015.

(45) Peng, K.-J.; Lai, J.-Y.; Liu, Y.-L. Preparation of Poly (Styrenesulfonic Acid) Grafted Nafion with a Nafion-Initiated Atom Transfer Radical Polymerization for Proton Exchange Membranes. *RSC Adv.* **2017**, *7*, 37255–37260.

(46) Si, K.; Dong, D.; Wycisk, R.; Litt, M. Synthesis and Characterization of Poly (Para-Phenylene Disulfonic Acid), its Copolymers and Their n-Alkylbenzene Grafts as Proton Exchange Membranes: High Conductivity at Low Relative Humidity. *J. Mater. Chem.* **2012**, *22*, 20907–20917.

(47) Wang, C.; Shin, D. W.; Lee, S. Y.; Kang, N. R.; Robertson, G. P.; Lee, Y. M.; Guiver, M. D. A Clustered Sulfonated Poly (Ether Sulfone) Based on a New Fluorene-Based Bisphenol Monomer. *J. Mater. Chem.* **2012**, *22*, 25093–25101.

(48) Silva, R.; De Francesco, M.; Pozio, A. Tangential and normal conductivities of Nafion® membranes used in polymer electrolyte fuel cells. *J. Power Sources* **2004**, *134*, 18–26.

(49) Roberti, E.; Carlotti, G.; Cinelli, S.; Onori, G.; Donnadio, A.; Narducci, R.; Casciola, M.; Sganappa, M. Measurement of the Young's Modulus of Nafion Membranes by Brillouin Light Scattering. *J. Power Sources* **2010**, *195*, 7761–7764.

(50) Caire, B. R.; Vandiver, M. A.; Pandey, T. P.; Herring, A. M.; Liberatore, M. W. Accelerated Mechanical Degradation of Anion Exchange Membranes via Hydration Cycling. *J. Electrochem. Soc.* **2016**, *163*, H964.

(51) Jung, H.-Y.; Kim, J. W. Role of the Glass Transition Temperature of Nafion 117 Membrane in the Preparation of the Membrane Electrode Assembly in a Direct Methanol Fuel Cell (DMFC). *Int. J. Hydrog. Energy* **2012**, *37*, 12580–12585.

(52) Meyer, Q.; Mansor, N.; Iacoviello, F.; Cullen, P.; Jervis, R.; Finegan, D.; Tan, C.; Bailey, J.; Shearing, P.; Brett, D. Investigation of Hot Pressed Polymer Electrolyte Fuel Cell Assemblies via X-Ray Computed Tomography. *Electrochim. Acta* **2017**, *242*, 125–136.

(53) Lage, L.; Delgado, P.; Kawano, Y. Thermal Stability and Decomposition of Nafion[®] Membranes with Different Cations. *J. Therm. Anal. Calorim.* **2004**, *75*, 521–530.

(54) Samms, S.; Wasmus, S.; Savinell, R. Thermal Stability of Nafion[®] in Simulated Fuel Cell Environments. *J. Electrochem. Soc.* **1996**, *143*, 1498.

(55) Mukaddam, M.; Litwiller, E.; Pinna, I. Gas Sorption, Diffusion, and Permeation in Nafion. *Macromolecules* **2016**, *49*, 280–286.

(56) Fan, Y.; Tongren, D.; Cornelius, C. J. The Role of a Metal Ion within Nafion upon its Physical and Gas Transport Properties. *Eur. Polym. J.* **2014**, *50*, 271–278.

(57) Chiou, J. S.; Paul, D. R. Gas Permeation in a Dry Nafion Membrane. *Ind. Eng. Chem. Res.* **1988**, *27*, 2161–2164.

(58) Lowry, S.; Mauritz, K. An Investigation of Ionic Hydration Effects in Perfluorosulfonate Ionomers by Fourier Transform Infrared Spectroscopy. *J. Am. Chem. Soc.* **1980**, *102*, 4665–4667.

(59) Huan, T. D.; Mannodi-Kanakkithodi, A.; Kim, C.; Sharma, V.; Pilania, G.; Ram-prasad, R. A Polymer Dataset for Accelerated Property Prediction and Design. *Sci. Data* **2016**, *3*, 160012.

(60) Kamal, D.; Tran, H.; Kim, C.; Wang, Y.; Chen, L.; Cao, Y.; Joseph, V. R.; Ram-prasad, R. Novel High Voltage Polymer Insulators using Computational and Data-Driven Techniques. *J. Chem. Phys.* **2021**, *154*, 174906.

(61) Kamal, D.; Wang, Y.; Tran, H. D.; Chen, L.; Li, Z.; Wu, C.; Nasreen, S.; Cao, Y.; Ramprasad, R. Computable Bulk and Interfacial Electronic Structure Features as Proxies for Dielectric Breakdown of Polymers. *ACS Appl. Mater. Interfaces* **2020**, *12*, 37182–37187.

(62) Weininger, D. SMILES, a Chemical Language and Information System. 1. Introduction to Methodology and Encoding Rules. *J. Chem. Inf. Comput. Sci.* **1988**, *28*, 31–36.

(63) Pilania, G.; Wang, C.; Jiang, X.; Rajasekaran, S.; Ramprasad, R. Accelerating Materials Property Predictions using Machine Learning. *Sci. Rep.* **2013**, *3*, 2810.

(64) Huan, T. D.; Mannodi-Kanakkithodi, A.; Ramprasad, R. Accelerated Materials Property Predictions and Design using Motif-Based Fingerprints. *Phys. Rev. B* **2015**, *92*, 014106.

(65) Mannodi-Kanakkithodi, A.; Pilania, G.; Huan, T. D.; Lookman, T.; Ramprasad, R. Machine Learning Strategy for the Accelerated Design of Polymer Dielectrics. *Sci. Rep.* **2016**, *6*, 20952.

(66) Rasmussen, C. E., Williams, C. K. I., Eds. *Gaussian Processes for Machine Learning*; The MIT Press: Cambridge, MA, 2006.

(67) Williams, C. K. I.; Rasmussen, C. E. In *Advances in Neural Information Processing Systems 8*; Touretzky, D. S., Mozer, M. C., Hasselmo, M. E., Eds.; MIT Press, 1995.

(68) Patra, A.; Batra, R.; Chandrasekaran, A.; Kim, C.; Huan, T. D.; Ramprasad, R. A multi-fidelity information-fusion approach to machine learn and predict polymer bandgap. *Comput. Mater. Sci.* **2020**, *172*, 109286.

(69) Kuenneth, C.; Rajan, A. C.; Tran, H.; Chen, L.; Kim, C.; Ramprasad, R. Polymer Informatics with Multi-Task Learning. *Patterns* **2021**, *2*, 100238.

(70) Tran, H.; Kim, C.; Gurnani, R.; Hvidsten, O.; DeSimpliciis, J.; Ramprasad, R.; Gadelrab, K.; Tuffle, C.; Molinari, N.; Kitchaev, D. et al. Polymer composites informatics for flammability, thermal, mechanical and electrical property predictions. *Polym. Chem.* **2025**, *16*, 3459–3467.

(71) TSCA Chemical Substance Inventory. <https://www.epa.gov/tsca-inventory>.

(72) Tingle, B. I.; Tang, K. G.; Castanon, M.; Gutierrez, J. J.; Khurelbaatar, M.; Dan-darchuluun, C.; Moroz, Y. S.; Irwin, J. J. ZINC-22 – A free multi-billion-scale database of tangible compounds for ligand discovery. *J. Chem. Inf. Model.* **2023**, *63*, 1166–1176.

(73) Mayr, A.; Klambauer, G.; Unterthiner, T.; Steijaert, M.; Wegner, J. K.; Ceulemans, H.; Clevert, D.-A.; Hochreiter, S. Large-scale comparison of machine learning methods for drug target prediction on ChEMBL. *Chem. Sci.* **2018**, *9*, 5441–5451.

(74) eMolecules. <https://www.emolecules.com/>.

(75) Matmerize, Inc., PolymRize. <https://polymrize.matmerize.com/>.

(76) McGrath, E., James; Hickner, M.; Wang, F.; Kim, Y.-S. Ion-conducting sulfonated polymeric materials. Patent EP1327278B1, 2001.

(77) Mirfarsi, S. H.; Kumar, A.; Jeong, J.; Brown, E.; Adamski, M.; Jones, S.; Mcdermid, S.; Britton, B.; Kjeang, E. Mechanical durability of reinforced sulfo-phenylated polyphenylene-based proton exchange membranes: Impacts of ion exchange capacity and reinforcement thickness. *J. Power Sources* **2025**, *630*, 236137.

(78) Mirfarsi, S. H.; Kumar, A.; Jeong, J.; Adamski, M.; McDermid, S.; Britton, B.; Kjeang, E. Thermo-Mechanical Stability of Hydrocarbon-Based Pemion® Proton Exchange Membranes. Electrochemical Society Meeting Abstracts 244. 2023; pp 1903–1903.

(79) Petreanu, I.; Ebrasu, D.; Sisu, C.; Varlam, M. Thermal analysis of sulfonated polymers tested as polymer electrolyte membrane for PEM fuel cells. *J. Therm. Anal. Calorim.* **2012**, *110*, 335–339.

(80) Ionomr Innovations Inc., *Pemion Safety data sheet (DSC)*; 2021; FM-7009-H, Document ID: FM-7009-H.

(81) García-Salaberri, P. A. Proton exchange membranes for polymer electrolyte fuel cells: An analysis of perfluorosulfonic acid and aromatic hydrocarbon ionomers. *Sustain. Mater. Technol.* **2023**, *38*, e00727.

(82) Kruczek, B. *Polyphenylene Oxide and Modified Polyphenylene Oxide Membranes: Gas, Vapor and Liquid Separation*; Springer, 2001; pp 61–104.

(83) Shiino, K.; Otomo, T.; Yamada, T.; Arima, H.; Hiroi, K.; Takata, S.; Miyake, J.; Miyatake, K. Structural investigation of sulfonated polyphenylene ionomers for the design of better performing proton-conductive membranes. *ACS Appl. Polym. Mater.* **2020**, *2*, 5558–5565.